



Analysis of Macular Pigment Optical Density in Macular Holes with Different Border Phenotypes

Alberto Quarta · Matteo Gironi · Maria Ludovica Ruggeri ·
Annamaria Porreca · Rossella D'Aloisio · Lisa Toto · Marta Di Nicola ·
Rodolfo Mastropasqua

Received: September 21, 2023 / Accepted: December 13, 2023 / Published online: January 4, 2024
© The Author(s) 2024

ABSTRACT

Introduction: We conducted a cross-sectional study to compare macular pigment optical density (MPOD) in eyes with idiopathic macular holes with bumpy (bbMH) and smooth borders (sbMH) and to assess the relation between MPOD and optical coherence tomography findings. Thirty eyes from thirty patients affected by idiopathic macular hole were studied.

Methods: All patients underwent SD-OCT and macular pigment optical density (MPOD) analysis. Comparison between the two border phenotypes were estimated at baseline, as well as the differences in MPOD, minimum and basal hole diameter, tractional hole index (THI), macular hole index (MHI), diameter hole index

(DHI), and ELM integrity metrics between the two groups.

Results: The mean MPOD was 0.09 ± 0.08 in bbMHs and 0.16 ± 0.11 in sbMHs ($p = 0.010$). Correlation analysis between MPOD and minimum hole diameter revealed a negative association ($\rho = -0.707$, $p = 0.008$) in bbMH and a positive association ($\rho = 0.702$, $p = 0.019$) in sbMH. MPOD and basal diameter were negatively correlated in bbMH ($\rho = -0.77$, $p = 0.001$) and positively correlated in sbMH ($\rho = 0.675$, $p = 0.019$). Indeed, MPOD is negatively correlated with THI and MHI in sbMH ($\rho = -0.684$, $p = 0.019$; $\rho = -0.665$, $p = 0.019$, respectively) and positively correlated in bbMH ($\rho = 0.593$, $p = 0.037$; $\rho = 0.658$, $p = 0.018$, respectively).

Conclusions: MPOD is significantly reduced in bbMHs compared to sbMHs. The two border phenotypes also differ for tractional and tangential indexes, possibly reflecting a different pathogenesis. Further studies are needed to understand the prognostic role of MPOD.

Marta Di Nicola and Rodolfo Mastropasqua contributed equally to this work.

A. Quarta (✉) · M. Gironi · M. L. Ruggeri ·
R. D'Aloisio · L. Toto · R. Mastropasqua
Department of Sciences, Ophthalmology Clinic,
National Center of High Technology in
Ophthalmology, Gabriele D'Annunzio University,
Via dei Vestini, 66100 Chieti, Italy
e-mail: alberto.quarta.96@gmail.com;
alberto.quarta@studenti.unich.it

A. Porreca · M. Di Nicola
Laboratory of Biostatistics, Department of Medical,
Oral and Biotechnological Sciences, University "G.
d'Annunzio" Chieti-Pescara, via dei Vestini 31,
66100 Chieti, Italy

Keywords: Macular hole; Muller cell cone;
Macular pigment; Macular hole borders

Key Summary Points

Why carry out this study?

Müller cell cones are involved in the idiopathic macular hole development with a possible role in foveal integrity.

This study was aimed at describing differences in macular pigment optical density (MPOD) as a surrogate measure of Müller cell cone involvement in two borders phenotypes' macular holes.

What was learned from the study?

Observing features of eyes with different macular hole borders and retinal layers involved in optical coherence tomography (OCT), we find new correlations between OCT features and MPOD, possibly reflecting residual Müller cell cone.

Since Müller cell cone is the primary cytotype that package macular pigment such as xanthophylls, surgical and therapeutic approaches can differ between the two macular hole phenotypes, particularly concerning possible new therapies for better anatomical and functional post-surgical recovery.

photoreceptor between bumpy (bbMH) and smooth borders (sbMH), impacting post-operative retinal layers restoration and visual acuity [3].

Comprehension of the foveal structure has provided more accurate details about its development and post-surgical closure. Notably, Yamada proposed that the Müller cells in the central fovea provide structural support to the foveal cones [4].

Müller cell cone (MCC) was proposed by Gass in 1999, who defined the shape, location, and possible roles of these cells as reservoir for retinal xanthophyll and primary structural support of the fovea. It appears to have a pivotal role in age-related macular degeneration and in the pathognomonic biomicroscopic aspect of foveomacular schisis [5].

Xanthophylls and zeaxanthin make foveal macular pigment. A reliable quantification of foveal macular pigment in vivo is provided by heterochromatic flicker photometry (HFP), in terms of macular pigment optical density (MPOD) [6–8]. MCC is crucial to maintain foveal integrity and macular pigment storage, easily measured by HFP. Several works have already demonstrated that MPOD is altered in vitreomacular interface disorders, given its role in foveal structural integrity [9, 10]. In this study, we assessed both sbMH and bbMH, exploring differences in MPOD, quantitative OCT metrics, and correlations between the two.

INTRODUCTION

Since Gass staged macular hole (MH) for the first time in 1988 by using biomicroscopy, essential findings related to the development and progression of MH have been described by using optical coherence tomography (OCT) [1]. Many studies reported macular hole structural characteristics, and the role of tangential and anteroposterior tractional forces was also investigated [2].

Recently, Govetto et al. analyzed in a retrospective study two different macular hole border patterns, underlining a different loss of

METHODS

This cross-sectional comparative study included thirty eyes from thirty patients with idiopathic full-thickness macular hole enrolled at University G. D'Annunzio, Chieti-Pescara, Italy, between August 2022 and April 2023. This study was approved by the institutional review board in adherence to tenets of the Declaration of Helsinki. Informed consent was obtained from all participants.

All patients underwent complete ophthalmological examination, including best-corrected visual acuity (BCVA) measurement expressed in the logarithm of the minimum

angle of resolution (logMAR), intraocular pressure (IOP) measurement with Goldman applanation tonometry, fundus examination with indirect ophthalmoscopy after 1% tropicamide instillation, multimodal imaging with optical coherence tomography (OCT) and macular pigment optical density (MPOD) quantification with heterochromatic flicker photometry (HFP) at the day of the first visit. Axial length was measured using partial coherence laser interferometry (IOL Master 700; Carl Zeiss Meditec, Jena, Germany). All the imaging was performed by a single trained ophthalmologist (AQ).

In addition to fundus examination, cataract staging was done according to the Lens Opacification Classification System III (LOCS III) by a single expert vitreoretinal surgeon (RM), after pharmacological mydriasis.

Exclusion criteria were: (1) prior intraocular surgery, (2) secondary full-thickness macular hole, high myopia (AxL > 26 mm), age-related macular degeneration, retinal vascular diseases, and uveitis (3) glaucoma and other optic neuropathies, (4) a cataract stage > NO2-NC2 or > C2 or > P2 according to LOCS III. Since many works disagree about how cataract surgery affects MPOD measured using HFP [11, 12], patients with pseudophakic eyes were excluded. Another exclusion criterion was the duration of symptoms > 6 months. Assessment of fixation was performed as previously described by Neelam et al. [13]. Briefly, fixation assessment was performed during slit-lamp biomicroscopic funduscopy, with a tiny slit-lamp beam projected onto the fovea. The patient was instructed to fixate the light beam's upper end. When the observer concluded that the fovea and the superior extremity of the slit-lamp beam coincided, the fixation was considered foveal.

IMAGING

All eyes underwent multimodal imaging examination with the same spectral domain OCT (SD-OCT) Spectralis HRA + OCT imaging device, with OCT Angiography Module (Heidelberg Engineering, Heidelberg, Germany) taking a 30° radial and detail (97

scans × 60 μm) scan centered on the macular hole.

The MP Screener II (Elektron Technology, Cambridge, United Kingdom) assessed the macular pigment optical density. MPOD values are provided on a scale of 0 to 1, so the lower the value, the higher the level of blue light hitting the foveal cones. Patients underwent a screening fixation test before examination and only those patients with a stable fixation were included in the study.

During the HFP exam, the instrument presents two flicker wavelengths, one of the blue (465 nm) and one other of the green (530 nm). The exam starts with a flickering rate higher than the critical flicker fusion rate, gradually reducing frequency to 6 Hz/s. The patient is required to make flicker matches using the two wavelength length by pressing a button as soon as flicker is detected. The process is repeated for different green–blue luminance ratios.

Detailed test mode was the pattern of choice, by testing the central and peripheral area: the former having a 1° circular central target and the latter during which the patient fixates on a larger 1.75° red spot located at 8° horizontal nasal eccentricity.

The instrument calculates MPOD as the log ratio of the central to the peripheral blue light luminance corresponding to the minimal flicker frequency perceived. Only the “accept” outcome given by the software was used for further analysis. Every test was repeated twice (with a 30-min interval between measurements) to verify the instrument's repeatability.

IMAGE ANALYSIS

Full-thickness macular holes were classified according to the International Vitreomacular Study Group Consensus (IVTS) [14].

All linear measurements were performed by selecting a horizontal line scan from radial acquisition centered at the hole center. MH borders were qualitatively defined by two graders (AQ, MG) according to Govetto et al.'s definition [3], and if agreement was not reached, a third senior grader was consulted (RM) (Fig. 1).

By using the built-in caliper tool from Heidelberg, several parameters were evaluated: hole minimum diameter, defined as the minimum horizontal distance between each edge of the hole; ellipsoid zone (EZ) defect, defined as the distance between EZ terminals on each side of the hole, external limiting membrane (ELM) to hole base distance (ELM_base) defined as the perpendicular distance between the ELM ending and RPE, measured nasally and temporally; ELM to hole edge (ELM_edge) distance defined as the shortest distance between ELM ending and the hole edge along the direction of the ELM, measured nasally and temporally; basal diameter distance. Additional parameters were obtained as previously described by Ruiz-Moreno et al. [2], so tractional hole index (THI), macular hole index (MHI), and diameter hole index (DHI) were calculated as a surrogate measure of tractional and tangential forces. Briefly, THI is defined as the ratio of the maximal MH height to the minimum diameter, MHI is defined as the ratio of the MH height to the diameter of the base, DHI is defined as the ratio of MH minimum diameter to the base diameter,

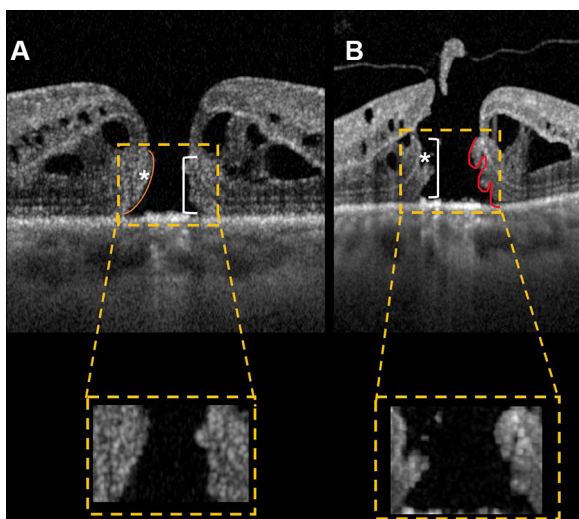


Fig. 1 Optical coherence tomography scans showing macular holes with smooth border (A) and bumpy border (B). Lumps of bumpy border macular holes are clearly distinguishable, suggesting a deeper cellular damage. ELM to hole base and ELM to hole edge are indicated in figure (*line* and *asterisk*, respectively)

STATISTICAL ANALYSIS

Assuming a pooled standard deviation of 0.09 units for MPOD, the study would require a sample size of 13 subjects or each group (i.e., a total sample size of 26, assuming equal group sizes) to achieve a power of 80% and a level of significance of 5% (two-sided), for detecting a true difference in means between groups (bbMH vs. sbMH). All statistical analyses were performed using Statistical Package for Social Sciences (version 22.0; SPSS Inc, Chicago, IL, USA) and R environment (version 4.1; <http://www.r-project.org/>). Descriptive statistics included frequencies and percentages for categorical variables and mean \pm standard deviation (SD) for quantitative ones. Nonparametric methods were preferred according to sample size. The differences between subjects with macular holes with bumpy and smooth borders were evaluated using a non-parametric unpaired *t* test (Mann–Whitney test). Spearman rank correlation coefficient (ρ) was used to investigate the relationships between MPOD and OCT metrics. Correction for multiple testing was performed by the Bonferroni method. All *p* values were two-tailed, and a *p* value ≤ 0.05 was considered statistically significant.

RESULTS

Characteristics of Patients Included in the Analysis

Of the 45 eyes initially screened for the study, only 30 filled the inclusion criteria, with 15 eyes showing bumpy borders macular holes and 15 showing smooth borders macular holes (Fig. 2).

Tables 1 and 2 show the results of the study.

Optical Coherence Tomography Metrics

Among our patients, 13 (43%) had small macular holes ($< 250 \mu\text{m}$), six (20%) were medium macular holes ($> 250 \mu\text{m}$ and $< 400 \mu\text{m}$), and 11 (37%) were large macular holes ($> 400 \mu\text{m}$).

The mean MPOD value was lower in the bbMH group respect sbMH (0.09 ± 0.08 vs. 0.16 ± 0.11 , $p = 0.010$) (Table 1, Fig. 3).

For tractional and tangential indexes, mean value for THI, MHI, and DHI were higher in the sbMH while the bbMH group had a wider EZ defect (Table 1). As concern for ELM metrics, ELM_base nasal was lower in sbMH while ELM_base temporal was nearly the same between two groups. The ELM_edge nasal was higher in sbMH, and mean ELM_edge temporal was higher in bbMH (300.67 ± 137.97 vs. 143.53 ± 71.75 , $p = 0.002$). The correlation analysis between MPOD and OCT metrics is illustrated in Table 2 both for sbMH and bbMH.

DISCUSSION

In this cross-sectional study, we demonstrated quantitative MPOD and structural OCT differences in bbMH and sbMH eyes. Comparing the two MH border phenotypes, sbMHs showed higher MPOD. Differences in residual macular pigment may reflect MCC survivors suggesting different foveal damage, potentially impacting post-surgical recovery. MCC plays a pivotal role in foveolar photoreceptor packaging, and its absence might make cones more susceptible to disruption at the umbo [5]. Higher MPOD in sbMHs may highlight MCC’s structural role against tangential and tractional forces. Obana et al. reported macular pigment distribution in MH at different stages, demonstrating its presence in the retinal flap in stage 2, in outer plexiform layers, and the operculum in stage 3,

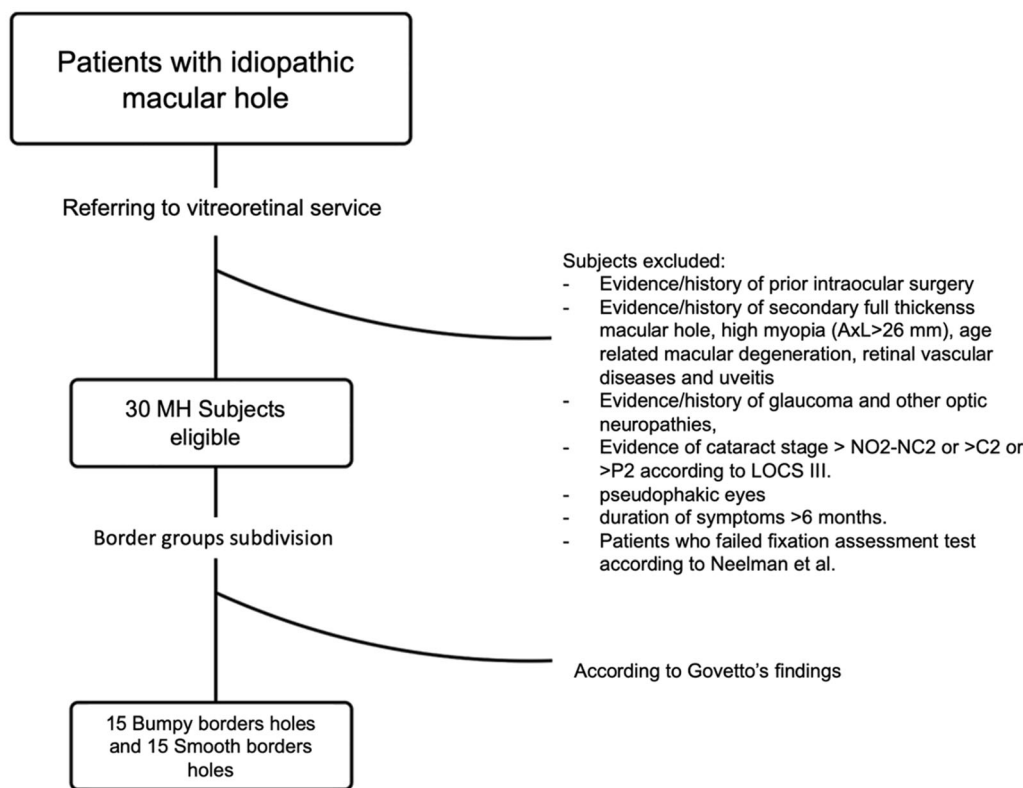


Fig. 2 Flowchart diagram describing the selection process of eligible patients for MH analysis. Only 30 patients were eligible for multimodal imaging evaluation starting from

initial cohort of subjects with idiopathic full thickness macular hole, referred to the vitreoretinal service

Table 1 Mean \pm SD for macular holes with bumpy (bbMH) and smooth borders (sbMH)

	bbMH ($n = 15$)	sbMH ($n = 15$)	p value
Age (years)	67.87 \pm 7.68	71.13 \pm 5.72	0.305
VA (logMAR)	0.78 \pm 0.14	0.60 \pm 0.10	0.004
Hole minimum diameter (μm)	432.33 \pm 170.13	257.67 \pm 90.25	0.011
Basal diameter (μm)	1411.80 \pm 346.11	658.47 \pm 259.14	< 0.001
MPOD	0.09 \pm 0.08	0.16 \pm 0.11	0.010
THI	1.34 \pm 0.97	1.75 \pm 0.61	0.011
MHI	0.35 \pm 0.14	0.75 \pm 0.26	< 0.001
DHI	0.32 \pm 0.08	0.41 \pm 0.97	0.016
EZ defect (μm)	2050.93 \pm 652.39	1454.67 \pm 333.10	0.029
ELM to hole base nasal (μm)	168.07 \pm 73.29	102.53 \pm 31.28	0.006
ELM to hole base temporal (μm)	108.20 \pm 52.92	107.33 \pm 48.86	0.098
ELM to hole edge nasal (μm)	115.87 \pm 50.13	438.93 \pm 432.87	0.041
ELM to hole edge temporal (μm)	300.67 \pm 137.97	143.53 \pm 71.75	0.002

MPOD macular pigment optical density, *THI* tractional hole index, *MHI* macular hole index, *DHI* diameter hole index, *VA* visual acuity, *EZ* ellipsoid zone, *ELM* external limiting membrane
 p value derived from Mann–Whitney U test

but also in the outer plexiform layers surrounding cystic spaces in stage 3 and 4 [10]. Bottoni et al. reported no improvement in visual acuity with revisualization of macular pigment after surgery and a nearly significant association of MPOD with ELM recovery during follow-up, possibly representing a phenomenon that merely accompanies the reapposition of the edges and their integrity [11].

Relating MPOD and ELM metrics, we found stronger negative correlations between MPOD and ELM_base distance in bbMHs. These results suggest that different inner retinal forces are transmitted to the outer retina through the MCC, resulting in outer retinal traction and ELM elevation. More profound damage in MCC may allow a higher ELM_base, potentially impacting post-surgical healing. Geenen et al. reported in a retrospective study that ELM height varies widely in MHs, with higher values in wider MHs and when the hole is higher [15]. Further support is given by Hangai et al., who demonstrated through three-dimensional

imaging of MH that the MCC truncated apex was located at the ELM, describing an inverted cone-shaped structure seen over the crown-shaped ends of the disrupted ELM [16]. MPOD negatively correlates with minimum and basal hole diameters in bbMHs and positively correlates with the two parameters in sbMHs. These results may reflect the width and location of the initial central retinal dehiscence influencing MCC disruption, with potential consequences on surgical outcomes. MCC's importance in MH development was explained by Cheung and Byeon's theory [17], distinguishing two MH types based on MCC and Z-shape Müller cell involvement. Low residual MPOD reflecting MCC survivor may result from a very disruptive process in bbMHs, and higher residual MPOD positively correlating with these linear metrics in sbMHs may suggest a residual structural role.

Macular pigment showed different behavior when considering tractional indexes, with positive correlations in bbMHs and negative correlations in sbMHs. These results further confirm

Table 2 Results of correlation analysis between MPOD and other variables in bumpy (bbMH) and smooth macular (sbMH) hole borders

	MPOD			
	bbMH		sbMH	
	rho	<i>p</i> value*	rho	<i>p</i> value*
VA (logMAR)	0.227	0.508	0.318	0.299
Minimum hole diameter (μm)	– 0.707	0.008	0.702	0.019
Basal diameter (μm)	– 0.775	0.001	0.675	0.019
EZ defect (μm)	– 0.035	0.901	0.303	0.299
ELM_baseN (μm)	– 0.717	0.008	– 0.512	0.080
ELM_baseT (μm)	– 0.171	0.597	– 0.609	0.029
ELM_edgeN (μm)	0.759	0.006	0.484	0.092
ELM_edgeT (μm)	– 0.420	0.164	0.634	0.024
THI	0.593	0.037	– 0.684	0.019
MHI	0.658	0.018	– 0.665	0.019
DHI	– 0.491	0.099	– 0.159	0.572

*Bonferroni adjusted

EZ ellipsoid zone, *THI* tractional hole index, *MHI* macular hole index, *DHI* diameter hole index, *VA* visual acuity, *EZ* ellipsoid zone, *ELM* external limiting membrane

Chung and Byeon's theory [17], suggesting that higher tractional forces are needed to obtain deeper foveolar damage in bbMHs. At the same time, sbMHs showed inverse correlations, indicating dehiscence type MH. Gass suggested that a yellow ring is visible in early phases due to MCC centrifugal migration caused by tangential vitreofoveal traction [18]. Innate differences in MCC amount in the foveola may explain different behavior, which leads to the two MH types and border patterns. The additional hypothesis could rely on MCC contact with the vitreous cortex during the action of tractional forces and uncertainty for which factors exactly dictate the width of the dehiscence zone at the onset. Residual MCC may play a potential role in the self-closure macular hole, as illustrated by Gass [18] and then investigated by Bringmann et al. [19]. Since we performed our clinical examination within six months of visual symptoms, it is also possible that among our cases, photoreceptor damage could have

occurred chronically or acutely as a direct consequence of MH formation. However, differentiating between the two is quite difficult in the clinical practice due to variability of patient's symptoms.

Our study has some limitations. First of all, the sample size is small given the relatively low incidence of macular hole. Additional difficulties derive from dividing the population into two groups according to border type. Moreover, initial fixation screening for eligible patients restricted the sample. Secondly, although B-scan images were adequate to assess border type, additional 3D techniques are required for a complete study. The exact time from macular hole formation is an additional issue since we do not know if the damage could be due to chronicity or tractional forces during hole development.

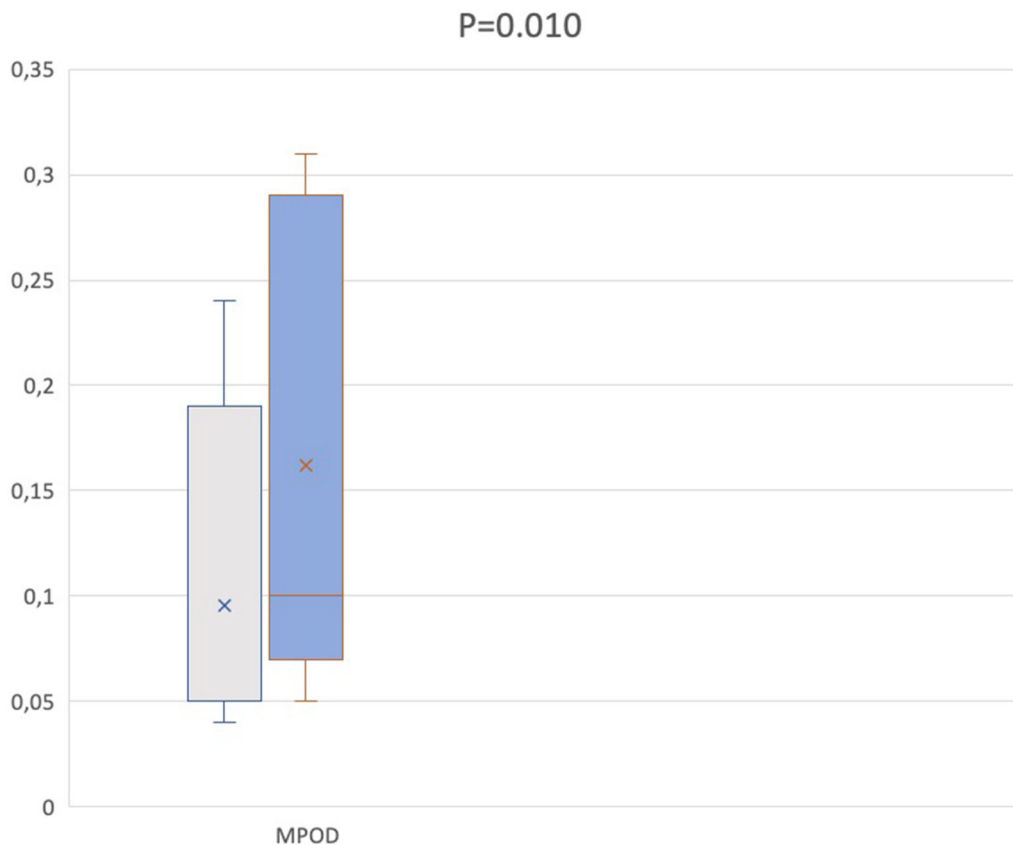


Fig. 3 Box-and-whisker plots showing analyzed MPOD measurements in bbMH and sbMH. Each box shows mean (*cross within the box*) and interquartile range (*horizontal extremes of the box*) values for MPOD in the two groups. The ends of the *whiskers* represent the minimum and

maximum values. Each graph (*gray* for bbMHs patients and *blue* for sbMHs patients, respectively) shows values of a different metric in each of the two groups. *P* values for comparison is reported. Details on pairwise comparisons are presented in Table 2

CONCLUSIONS

In conclusion, this study assessed MPOD in bbMHs and sbMHs, probably reflecting different damage to MCC. In addition, ELM_base might be a prognostic biomarker for post-surgical ELM recovery and MCC healing by macular pigment reaccumulation when considering the two border phenotypes. Further studies are needed to investigate MPOD and the potential role of MCC in MH self-closure.

Author Contribution. Alberto Quarta, Rodolfo Mastropasqua: concept and design. Alberto Quarta, Matteo Gironi, Lisa Toto, Rodolfo Mastropasqua: drafting the manuscript.

Alberto Quarta, Maria Ludovica Ruggeri, Rossella D'Aloisio: collecting data.

Funding. No funding or sponsorship was received for this study or publication of this article. The journal's Rapid Service Fee was funded by the authors.

Data Availability. The datasets used and/or analyzed during the current study available from the corresponding author on reasonable request.

Declarations

Conflict of interest. All named authors confirm they have no competing interests to declare.

Ethical Approval. This prospective study adhered to the 1964 Helsinki Declaration and its later amendments. All subjects signed an informed consent at the time of examination for prospective studies. Institutional Review Board Committee of Gabriele D’Annunzio University of Chieti-Pescara at SS. Annunziata Hospital approved this study (IRB NUMBER 1047 DNICS).

Open Access. This article is licensed under a Creative Commons Attribution-NonCommercial 4.0 International License, which permits any non-commercial use, sharing, adaptation, distribution and reproduction in any medium or format, as long as you give appropriate credit to the original author(s) and the source, provide a link to the Creative Commons licence, and indicate if changes were made. The images or other third party material in this article are included in the article’s Creative Commons licence, unless indicated otherwise in a credit line to the material. If material is not included in the article’s Creative Commons licence and your intended use is not permitted by statutory regulation or exceeds the permitted use, you will need to obtain permission directly from the copyright holder. To view a copy of this licence, visit <http://creativecommons.org/licenses/by-nc/4.0/>.

REFERENCES

- Gass JD. Idiopathic senile macular hole: its early stages and pathogenesis. 1988. *Retina*. 2003;23(6 Suppl):629–39.
- Ruiz-Moreno JM, Staicu C, Piñero DP, Montero J, Lugo F, Amat P. Optical coherence tomography predictive factors for macular hole surgery outcome. *Br J Ophthalmol*. 2008;92(5):640–4.
- Govetto A, Bacherini D, Romano MR, et al. Full-thickness macular hole: are supra-RPE granular deposits remnants of photoreceptors outer segments? Clinical implications. *Am J Ophthalmol*. 2023;245:86–101.
- Yamada E. Some structural features of the fovea centralis in the human retina. *Arch Ophthalmol*. 1969;82(2):151–9.
- Gass JD. Müller cell cone, an overlooked part of the anatomy of the fovea centralis: hypotheses concerning its role in the pathogenesis of macular hole and foveomacular retinoschisis. *Arch Ophthalmol*. 1999;117(6):821–3.
- van der Veen RL, Berendschot TT, Hendrikse F, Carden D, Makridaki M, Murray IJ. A new desktop instrument for measuring macular pigment optical density based on a novel technique for setting flicker thresholds. *Ophthalmic Physiol Opt*. 2009;29(2):127–37.
- Davey PG, Alvarez SD, Lee JY. Macular pigment optical density: repeatability, intereye correlation, and effect of ocular dominance. *Clin Ophthalmol*. 2016;10:1671–8.
- Obana A, Gohto Y, Moriyama T, Seto T, Sasano H, Okazaki S. Reliability of a commercially available heterochromatic flicker photometer, the MPS2, for measuring the macular pigment optical density of a Japanese population. *Jpn J Ophthalmol*. 2018;62(4):473–80.
- Bottoni F, Zanzottera E, Carini E, Cereda M, Cigada M, Staurenghi G. Re-accumulation of macular pigment after successful macular hole surgery. *Br J Ophthalmol*. 2016;100(5):693–8.
- Obana A, Nakazawa R, Noma S, Sasano H, Gohto Y. Macular pigment in eyes with macular hole formation and its change after surgery. *Transl Vis Sci Technol*. 2020;9(11):28 (Published 2020 Oct 26).
- Verdina T, Date P, Benatti C, et al. Evaluation of macular pigment optical density following femtosecond laser-assisted cataract surgery. *Clin Ophthalmol*. 2019;13:821–8.
- Gultekin BP, Bulut A, Bilen N, Kalayci D. Comparison of macular pigment optical density between phakic and pseudo-phakic eyes. *Biomed Res*. 2018;29:1653–6.
- Neelam K, O’Gorman N, Nolan J, O’Donovan O, Au Eong KG, Beatty S. Macular pigment levels following successful macular hole surgery. *Br J Ophthalmol*. 2005;89(9):1105–8.
- Duker JS, Kaiser PK, Binder S, et al. The International Vitreomacular Traction Study Group classification of vitreomacular adhesion, traction, and macular hole. *Ophthalmology*. 2013;120(12):2611–9.
- Geenen C, Murphy DC, Sandinha MT, Rees J, Steel DHW. Significance of preoperative external

- limiting membrane height on visual prognosis in patients undergoing macular hole surgery. *Retina*. 2019;39(7):1392–8.
16. Hangai M, Ojima Y, Gotoh N, et al. Three-dimensional imaging of macular holes with high-speed optical coherence tomography. *Ophthalmology*. 2007;114(4):763–73.
 17. Chung H, Byeon SH. New insights into the pathoanatomy of macular holes based on features of optical coherence tomography. *Surv Ophthalmol*. 2017;62(4):506–21.
 18. Gass JD. Reappraisal of biomicroscopic classification of stages of development of a macular hole. *Am J Ophthalmol*. 1995;119(6):752–9.
 19. Bringmann A, Duncker T, Jochmann C, Barth T, Duncker GIW, Wiedemann P. Spontaneous closure of small full-thickness macular holes: presumed role of Müller cells. *Acta Ophthalmol*. 2020;98(4):e447–56. <https://doi.org/10.1111/aos.14289>.